JOC Article

A Theoretical Study of the Mechanisms and Regiochemistry of the Reactions of 5-Alkoxyoxazole with Thioaldehydes, Nitroso Compounds, and Aldehydes

Zhi-Xiang Yu*,† and Yun-Dong Wu*

Department of Chemistry, The Hong Kong University of Science & Technology, Clearwater Bay, Kowloon, Hong Kong, China

zhixiang@chem.ucla.edu; chydwu@ust.hk

Received August 16, 2002

A theoretical study based on B3LYP/6-31G* calculations has been applied to the mechanisms and regiochemistry of reactions of 5-alkoxyoxazole with thioaldehydes, nitroso compounds, and aldehydes. All three reactions adopt similar mechanisms, which start with Diels−Alder (DA) reactions, followed by either a novel, concerted ring-opening−ring-closing (RORC) step to transfer the DA adduct to 2-alkoxycarbonyl-3-thiazoline and 2-alkoxycarbonyl-3-oxazoline for thioaldehydes and aldehydes, respectively, or stepwise ring-opening and ring-closing steps to generate 1,2,4-oxadiazoline for nitroso compounds. The reactions of 5-alkoxyoxazole with thioaldehydes and nitroso compounds can be conducted under thermal reaction conditions due to the 10 kcal/mol activation barriers for their rate-determining DA reactions. By contrast, the reaction of 5-alkoxyoxazole with aldehydes cannot take place under thermal conditions, since this bimolecular reaction has the rate-determining RORC transition state higher than the reactants by 30.5 kcal/mol.

1. Introduction

Oxazoles are reactive five-membered aromatic heterocyclic dienes that can participate in Diels−Alder (DA) reactions.[1] The thermal reactions of oxazoles with alkenes and with alkynes, for example, are widely used to synthesize substituted pyridines and furans, respectively.[1,2] In 1988, Vedejs and Fields observed that when alkoxyl groups were introduced to the C_5 atom of oxazole, the resulting 5-alkoxyoxazoles can trap the in situ generated thioaldehydes to produce 2-alkoxycarbonyl-3-thiazolines (on the contrary, both 5-alkyl and unsubstituted oxazoles cannot take part in such reactions) (Scheme 1, eq 1a).[3] Later, Suga and Ibata found that 5-alkoxyoxazoles can also react with nitrosobenzene to produce 1,2,4-oxadiazolines (Scheme 1, eq 1b).[4] The reactions of 5-alkoxyoxazoles with other dienophiles[5−7] have also been reported. Among them of synthetic importance is the Lewis acid-catalyzed reaction between 5-alkoxyoxazoles and aldehydes[6,7] (Scheme 1, eq 1c), since the generated 4-alkoxycarbonyl-2-oxazolines from these reactions can be easily transformed to the valuable organic intermediates *β*-hydroxy amino acids and 2-amino-1,3-diols.[8−11] Depending on the substrates, catalysts, and solvents used, the final 4-alkoxycarbonyl-2-oxazolines of reaction 1c can be dominated by conformers with either trans or cis R^1 and CO_2Me configurations (referred to here as *trans*- and *cis*-2-oxazolines). Due to the fact that *cis*-2-oxazolines can be produced through choosing appropriate catalysts, reaction 1c provides a complementary

† Present address: Department of Chemistry and Biochemistry, University of California, Los Angeles, CA 90095-1569. Fax: (310) 206-1843.

(1) For recent reviews, see: (a) Boger, D. L.; Weinreb, S. N. Hetero Diels−Alder Methodology in Organic Synthesis. *Organic Chemistry, A Series of Monographs*, Academic Press: New York, 1987; No. 47. (b) Maryanoff, B. E. In *Oxazoles*; Turchi, I. J., Ed.; *The Chemistry of Heterocyclic Compounds series*; Weissberger, A., Taylor, E. C., Eds.; Wiley-Interscience: New York, 1986; Vol. 45, p 963. (c) Turchii, I. J.; Dewar, M. J. S. *Chem. Rev.* **1975**, *75*, 389.

(2) (a) Jacobi, P. A.; Blum, C. A.; Desimone, R. W.; Udodong, U. E. S. *Tetrahedron Lett.* **1989**, *30*, 7173. (b) Whitney, S. C.; Rickborn, B. *J. Org. Chem.* **1988**, *53*, 5595.

(3) Vedejs, E.; Fields, S. *J. Org. Chem.* **1988**, *53*, 4663.

(4) Suga, H.; Ibata, T. *Chem. Lett.* **1991**, 1221.

(5) (a) Hassner, A.; Fisher, B. *Tetrahedron*, **1989**, *45*, 3535. (b) Suga, H.; Shi, X.; Ibata, T. *Chem. Lett.* **1994**, 1673.

(6) Suga, H.; Shi, X.; Fujieda, H.; Ibata, T. *Tetrahedron Lett.* **1991**, *32*, 6911. (b) Suga, H.; Shi, X.; Ibata, T. *J. Org. Chem.* **1993**, *58*, 7397. (c) Suga, H.; Ibata, T. *Tetrahedron Lett.* **1989**, *39*, 869. (d) Suga, H.; Ikai, K.; Ibata, T. *J. Org. Chem.* **1999**, *64*, 7040. (e) Suga, H.; Shi, X.; Ibata, T. *Bull. Chem. Soc. Jpn.* **1998**, *71*, 1231. (f) Suga, H.; Shi, X.; Ibata, T.; Kakehi, A. *Heterocycles* **2001**, *55*, 1711. (g) Suga, H.; Fujieda, H.; Hirotsu, Y.; Ibata, T. *J. Org. Chem.* **1994**, *59*, 3359. (h) For a recent review of these Lewis acid-catalyzed reactions, see: (i) Suga, H.; Ibata, T. *Reviews on Heteroatom Chemistry* **1999**, *21*, 195.

(7) Evans, D. A.; Janey, J. M.; Magomedov, N.; Tedrow, J. *Angew. Chem., Int. Ed.* **2001**, *40*, 1884.

(8) For a review of the syntheses of 4-alkoxycarbonyl-2-oxazoline using isocyanoacetates and conversion to *β*-hydroxyamine acids, see: Matsumoto, K.; Moriya, T.; Suzuki, M. J. *Synth. Org. Chem. Jpn.* **1988**, *43*, 7664.

(9) (a) Hoppe, D.; Schöllkopphf, U. *Justus Liebigs Ann. Chem.* **1972**, *763*, 1. (b) Matsumoto, K.; Urabe, Y.; Ozaki, Y.; Iwasaki, T.; Miyoshi, M. *Agric. Biol. Chem.* **1975**, *39*, 1869. (c) Matsumoto, K.; Ozaki, Y.; Suzuki, M.; Miyoshi, M. *Agric. Biol. Chem.* **1976**, *40*, 2045. (d) Ozaki, Y.; Matsumoto, K.; Miyoshi, M. *Agric. Biol. Chem.* **1978**, *42*, 1565.

(10) (a) Ito, Y.; Sawamura, M.; Hayashi, T. *J. Am. Chem. Soc.* **1986**, *108*, 6405. (b) Ito, Y.; Sawamura, M.; Hayashi, T. *Tetrahedron Lett.* **1987**, *28*, 6215; **1988**, *29*, 239. (c) Ito, Y.; Sawamura, M.; Shirakawa, E.; Hayashizaki, K.; Hayashi, T. *Tetrahedron Lett.* **1988**, *29*, 235. (d) Ito, Y.; Sawamura, M.; Shirakawa, E.; Hayashizaki, K.; Hayashi, T. *Tetrahedron* **1988**, *44*, 5253.

(11) The stereoselective synthesis of α-amino-*β*-hydroxy acids is an intensive research field, since these acids are building blocks of numerous peptide-based natural products including the vancomycin antibiotics; see references in ref 7.

10.1021/jo026330e CCC: $25.00
Published on Web 12/17/2002

SCHEME 1

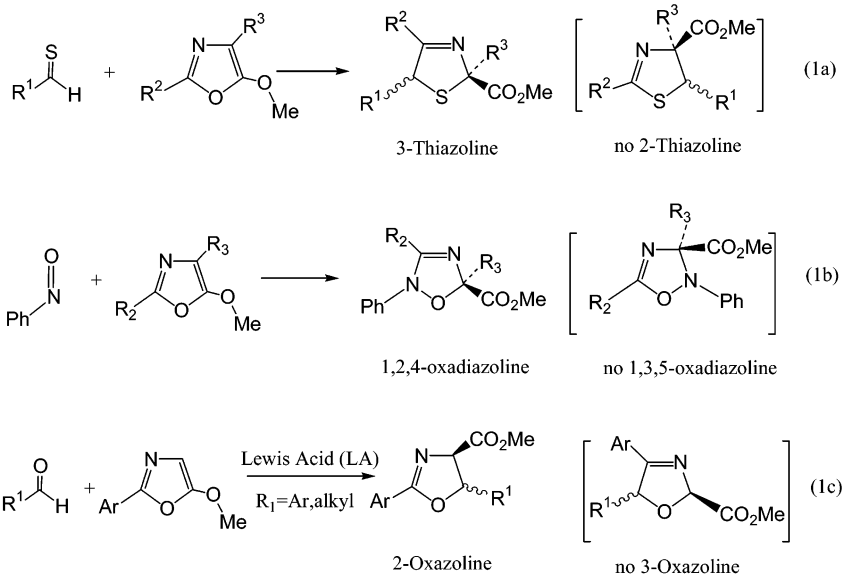

SCHEME 2

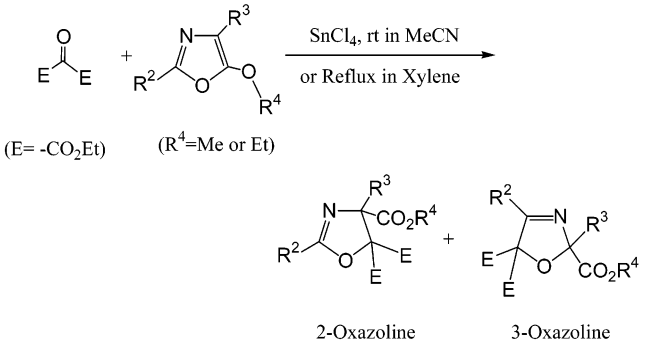

SCHEME 3

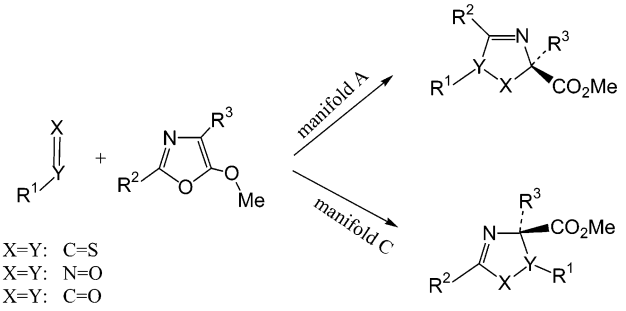

route to the aldol reaction between aldehydes and methylisocyanoacetates, which can only produce *trans*-2-oxazolines.[8] A very important development along this line is the highly enantioselective synthesis of *cis*-4-alkoxycarbonyl-2-oxazoline by applying chiral bulky Lewis acid (LA) catalysts, such as BINOL-AlMe by Suga and Ibata[6] or a Salen−aluminum complex by Evans and coworkers.[7]

The origin of the high cis-diastereoselectivity and enantioselectivity of reaction 1c when Evans's catalyst is used is not well-understood and is worthy of further investigation. In this and the companion paper, however, we address three other interesting questions.

The first question regards the different regiochemistry of reactions 1a−c. It was reported that reactions of 5-alkoxyoxazoles with oxomalonates usually generate a mixture of 2-alkoxycarbonyl-3-oxazolines and 4-alkoxycarbonyl-2-oxazolines and the ratio of the two isomers is dependent on the substituents and reaction conditions used (Scheme 2).[5] On the contrary, reactions 1a−c have specific regiochemistry to generate only one isomer: 3-thiazolines (instead of 2-thiazolines) for reaction 1a, 1,2,4-oxadiazolines (instead of 1,3,5-oxadiazolines) for reaction 1b, and 2-oxazolines (instead of 3-oxazolines) for reaction 1c (unless otherwise mentioned, 3- and 2-oxazolines in what follows are referred to as 2-alkoxycarbonyl-3-oxazoline and 4-alkoxycarbonyl-2-oxazoline, respectively; 2- and 3-thiazolines are defined similarly). It would be very interesting to know the factors that control the regiochemistry in reactions 1a−c; i.e., why do reactions 1a and 1b prefer manifold A to generate the product with the double bond in the 3−4 position of the 5-membered rings while reaction 1c produces final product via manifold C with a double bond in the 2−3 position of the five-membered ring (Scheme 3)?

The second question is about the role of the LA used in reaction 1c. It is not clear whether the different regiochemistry of reaction 1c compared to reactions 1a and 1b is caused by the LA and/or by substituent effects. Therefore, a comparison of the reactions of 5-alkoxyoxazoles and aldehydes, both in the presence and absence of LA, is expected to give us an in-depth insight of these reaction mechanisms.

The third question that intrigues us is about the origin of the cis-diastereoselectivity encountered in reaction 1c when bulky catalysts were used.[6,7]

To answer the above questions, detailed reaction mechanisms for reactions 1a−c were needed. Therefore, we investigated five model reactions shown in Scheme 4. The studies of reactions I−III will be presented with the purpose of knowing the detailed reaction mechanisms and intrinsic regio- and stereochemical features of reactions of 5-methoxyoxazole (MOX) with thioacetaldehyde $CH_3CH{=}S$, nitrosomethane ($CH_3N{=}O$), and acetaldehyde ($CH_3CH{=}O$). In addition, the study of reaction III can

SCHEME 4[a,b]

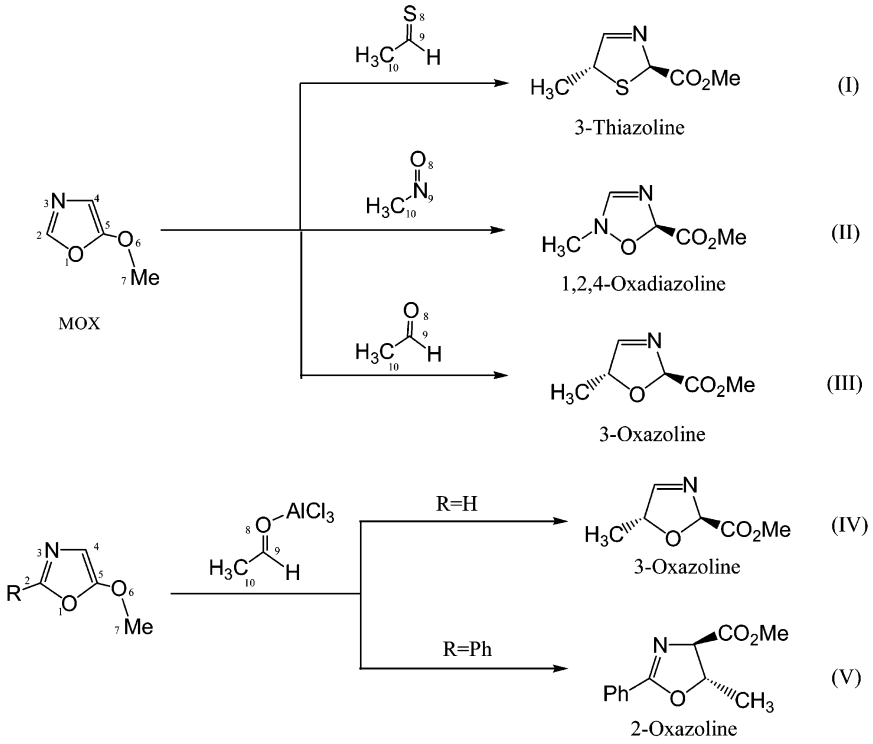

[a] Only the theoretically predicted major products are shown. [b]Only one diastereomer or enantiomer is shown for each reaction.

also serve to identify the reasons why this type of reaction cannot be conducted under thermal reaction conditions. The investigation of LA-catalyzed reactions (IV and V) is aimed to analyze the regio- and stereochemical characteristics in the presence of the LA. While the LAs used are $SnCl_4$, $TiCl_4$, $AlCl_2Me$, etc., to simplify the calculations and to extract the common features shared by different LAs in catalyzing these reactions, $AlCl_3$ is chosen as the catalyst during the theoretical modeling.

Our results indicate that the 5-alkoxyoxazoles react with thioacetaldehyde, nitrosomethane, and acetaldehyde with similar mechanisms (via manifold A) to give 3-thiazoline, 1,2,4-oxadiazoline, and 3-oxazoline, respectively (Scheme 5). The failure of applying thermal reaction conditions to the reaction between aldehyde and 5-alkoxyoxazole is primarily attributed to the high activation barrier needed to convert the Diels−Alder adduct to the final 3-oxazoline product [the ring-opening−ring closing (RORC) step; see Scheme 5]. When LA is used, the activation barrier of each step drops dramatically. Like the thermal reaction between aldehyde and 5-alkoxyoxazole, the LA-catalyzed reaction also intrinsically prefers to afford 3-oxazoline. Only when an aryl group is present at the C_2 position of 5-alkoxyoxazole does the final product become a 2-oxazoline (reaction V).

All the results will be addressed in this and the companion paper.[34] This paper will focus on the comparison of the reactions I−III to probe the intrinsic regiochemical propensity of thioaldehydes, nitroso compounds, and aldehydes when they react with 5-alkoxyoxazoles. The following paper, on the other hand, will be devoted to understand the regio- and stereochemical features of LA-catalyzed reactions of aldehydes with 5-alkoxyoxazoles. The origin of the regio- and enantioselectivity of reaction 1c caused by Evans' catalyst is the subject of ongoing theoretical investigation and will be reported in due course.

SCHEME 5

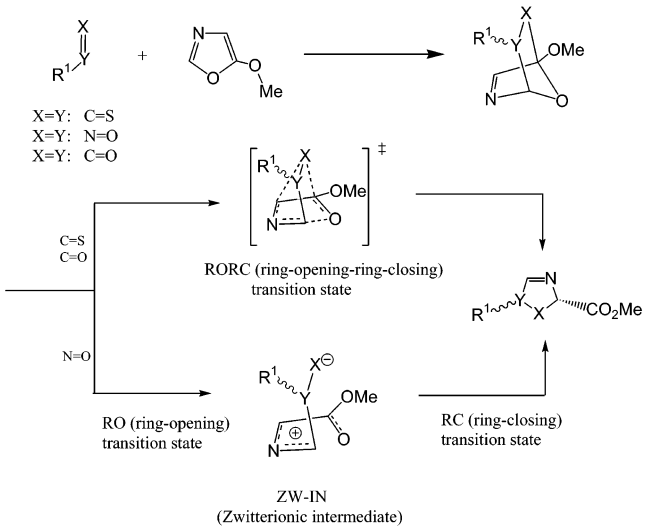

2. Computational Strategy and Methodology

Since reactions I−III, shown in Scheme 5, can be envisaged as being initiated by a DA reaction followed by some rearrangement processes, there are four possible manifolds, which differ from each other by the relative orientations of the diene MOX and heterodienophiles (Y═X) in the transition states, as illustrated in Scheme 6.[12] Manifolds A and B have the heterodienophiles attack the diene fragment C_2═N_3−C_4═C_5 of 5-alkoxyoxazole, whereas the C and D manifolds have the heterodienophiles attack the diene fragment of C_2═O_1−C_5═

SCHEME 6

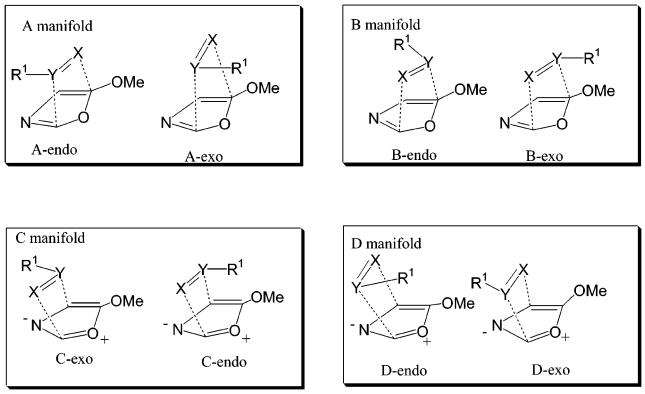

C_4, which is a resonance form of oxazole. Each manifold in reactions I−III has two paths, endo and exo, according to the orientation of the methyl group of the dienophiles in the DA transition states with respect to the diene fragments.

Due to the existence of a large number of paths as well as the possible stationary points involved, to save computation time without sacrificing the reliability of the calculations, all the possible reaction paths in reactions I−III were first searched at the Hartree−Fock level by using the HF/3-21G* method,[13] these calculations are provided in the Supporting Information. Then DFT calculations based on the B3LYP/6-31G* method[14−16] were carried out for the favored paths in each manifold. All structures were fully optimized, and frequency calculations were performed to determine the nature of each stationary point at both the HF and DFT levels. For TSs, intrinsic reaction coordinate (IRC)[17] calculations were used to follow reaction pathways. Moreover, motion of the imaginary frequencies of the transition structures was animated using MOLDEN[18] to ensure that the optimized stationary point corresponds to the transition structure of the desired reaction.

Our calculations indicate that the most favored manifold for reactions I−III is the A manifold. Therefore, we only report the results of A-endo and A-exo paths for these three reactions within this context. The energies and structures for other competing paths are given in Supporting Information for brevity.

Bond orders reported are the Wiberg bond indices[19a] calculated by means of natural bond orbital (NBO)[19b−c] analysis at the B3LYP/6-31G* level. The charges reported are NPA charges. Orbital energies are computed at the HF/6-31G* level upon the DFT structures. All calculations were carried out with the Gaussian 98 program package.[20]

3. Results

Unless otherwise mentioned, all the relative energies (kcal/mol) discussed are electronic energies including unscaled zero-point energy (ZPE) corrections (denoted as ΔE_0). The free energy, ΔG_{298}, is also provided for reference. In addition, the discussed stereochemical outcomes of reactions I−III are based on the assumption that these reactions are kinetically controlled.

Figure 1 depicts the frontier orbitals, NPA charges, as well as the DFT-optimized structures of the diene 5-methoxyoxazole (MOX) and the three heterodienophiles. Clearly, all three DA reactions between diene and dienophiles can be classified as normal electron-demand DA reactions[21] controlled mainly by the $HOMO_{diene}$ and the $LUMO_{dienophile}$, since the gap between $HOMO_{diene}$ and the $LUMO_{dienophile}$ in each case is smaller than the corresponding gap between $(HOMO\text{-}1)_{dienophile}$ and $LUMO_{diene}$ (the HOMOs of the heterodienophiles $CH_3CH{=}S$, $CH_3N{=}O$, and $CH_3CH{=}O$ lie in the plane of the double bond, corresponding to the lone pairs of the heteroatoms).

3.1. Reaction I (MOX + $CH_3CH{=}S$).

The potential energy surfaces for the A manifold are given in Figure 2. The computed structures of the stationary points involved in both A-endo and A-exo paths are provided in Figure S5 of the Supporting Information.

Figures 2 and S5 indicate that the A-endo/A-exo starts with a DA reaction via DA transition states (TSs) **1**/**5**, generating DA adducts **2**/**6**, followed by a novel, one-step RORC process via RORC TSs **3**/**7** to give rise to 3-thiazolines **4**/**8**. The DA reactions in both paths are concerted but asynchronous processes with more advanced C−C bond formation than C−S bond formation, as supported by IRC calculations. Bond orders of the forming C−C (∼0.4) and C−S (∼0.2) bonds in TS **1** (see the values in parentheses in Figure S5) also sustain this asynchronous character. Similar to the general endo selectivity for the DA reactions,[21b,22] the manifold A favors the endo TS **1** over the exo TS **5** with activation energies of 9.1 and 9.8 kcal/mol with respect to the reactants (MOX + $CH_3CH{=}S$), respectively. Houk[23] and Vedejes[24] also

(12) For reactions I−III, their possible pathways involving the nucleophilic attack of C_2 and C_4 of alkoxyoxazole to the Y atoms of dienophiles $CH_3Y{=}X$ can be ruled out, due to the fact that there are no corresponding nucleophilic attack transition states (TSs) of C_2 to Y atoms while the nucleophilic TSs of C_4 to Y are much higher in energies than their corresponding Diels−Alder TSs (see Figure S12 in the Supporting Information).

(13) Hehre, W. J.; Radom, L.; Schleyer, P. v. R.; Pople, J. A. *Ab Initio Molecular Orbital Theory*; Wiley: New York, 1986.

(14) (a) Becke, A. D. *J. Chem. Phys.* **1993**, *98*, 5648. (b) Lee, C.; Yang, W.; Parr, R. *Phys. Rev. B* **1988**, *37*, 785.

(15) For reviews of density-functional methods, see: (a) Parr, R. G.; Yang, W. *Density Functional Theory of Atoms and Molecules*; Oxford University Press: New York, 1989. (b) Ziegler, T. *Chem. Rev.* **1991**, *91*, 651. (c) *Density Functional Methods in Chemistry;* Labanowski, J., Andzelm, J., Eds.; Springer: Berlin, 1991.

(16) For discussion of using the DFT method in the study of pericyclic reactions, see: (a) Wiest, O.; Houk, K. N. *Top. Curr. Chem.* **1996**, *183*, 1 and reference therein. (b) Yu, Z.-X.; Dang, Q.; Wu, Y.-D. *J. Org. Chem.* **2001**, *66*, 6029.

(17) (a) Gonzalez, C.; Schlegel, H. B. *J. Chem. Phys.* **1989**, *90*, 2154. (b) Gonzalez, C.; Schlegel, H. B. *J. Phys. Chem.* **1990**, *94*, 2435.

(18) Schaftenaar, G.; Noordik, J. H. *J. Comput.-Alded Mol. Des.* **2000**, *14*, 123.

(19) (a) Wiberg, K. B. *Tetrahedron* **1968**, *24*, 1083. (b) Reed, A. E.; Weinstock, R. B.; Weinhold, F. *J. Chem. Phys.* **1985**, *83*, 735. (c) Reed, A. E.; Curtiss, L. A.; Weinhold, F. *Chem. Rev.* **1988**, *88*, 899.

(20) Frisch, M. J.; Trucks, G. W.; Schlegel, H. B.; Scuseria, G. E.; Robb, M. A.; Cheeseman, J. R.; Zakrzewski, V. G.; Montgomery, J. A.; Stratmann, R. E.; Burant, J. C.; Dapprich, S.; Millam, J. M.; Daniels, A. D.; Kudin, K. N.; Strain, M. C.; Farkas, O.; Tomasi, J.; Barone, V.; Cossi, M.; Cammi, R.; Mennucci, B.; Pomelli, C.; Adamo, C.; Clifford, S.; Ochterski, J.; Petersson, G. A.; Ayala, P. Y.; Cui, Q.; Morokuma, K.; Malick, D. K.; Rabuck, A. D.; Raghavachari, K.; Foresman, J. B.; Cioslowski, J.; Oritz, J. V.; Stefanov, B. B.; Liu, G.; Liashenko, A.; Piskorz, P.; Komaromi, I.; Gomperts, R.; Martin, R. L.; Fox, D. J.; Keith, T.; Al-Laham, M. A.; Peng, C. Y.; Nanayakkara, A.; Gonzalez, C.; Challacombe, M.; Gill, P. M. W.; Johnson, B. G.; Chen, W.; Wong, M. W.; Andres, J. L.; Head-Gordon, M.; Replogle, E. S.; Pople, J. A. *Gaussian 98, Revision A.1*; Gaussian, Inc.: Pittsburgh, PA, 1998.

(21) (a) Sustmann, R. *Tetrahedron Lett.* **1971**, 2721. (b) Sauer J.; Sustmann, R. *Angew. Chem., Int. Ed. Engl.* **1980**, *19*, 779.

(22) For a recent discussion of endo/exo selectivity in Diels−Alder reactions, see: (a) Carcia, J. I.; Mayoral, J. A.; Salvatella, L. *Acc. Chem. Res.* **2000**, *33*, 658. (b) Ujaque, G.; Lee, P. S.; Houk, K. N.; Hentemann, M. F.; Danishefsky, S. J. *Chem. Eur. J.* **2002**, *8*, 3423.

(23) (a) McCarrick, M. A.; Wu, Y.-D.; Houk, K. N. *J. Am. Chem. Soc.* **1992**, *114*, 1499. (b) McCarrick, M. A.; Wu, Y.-D.; Houk, K. N. *J. Org. Chem.* **1993**, *58*, 3330. (c) Leach, A. G.; Houk, K. N. *J. Org. Chem.* **2001**, *66*, 5192.

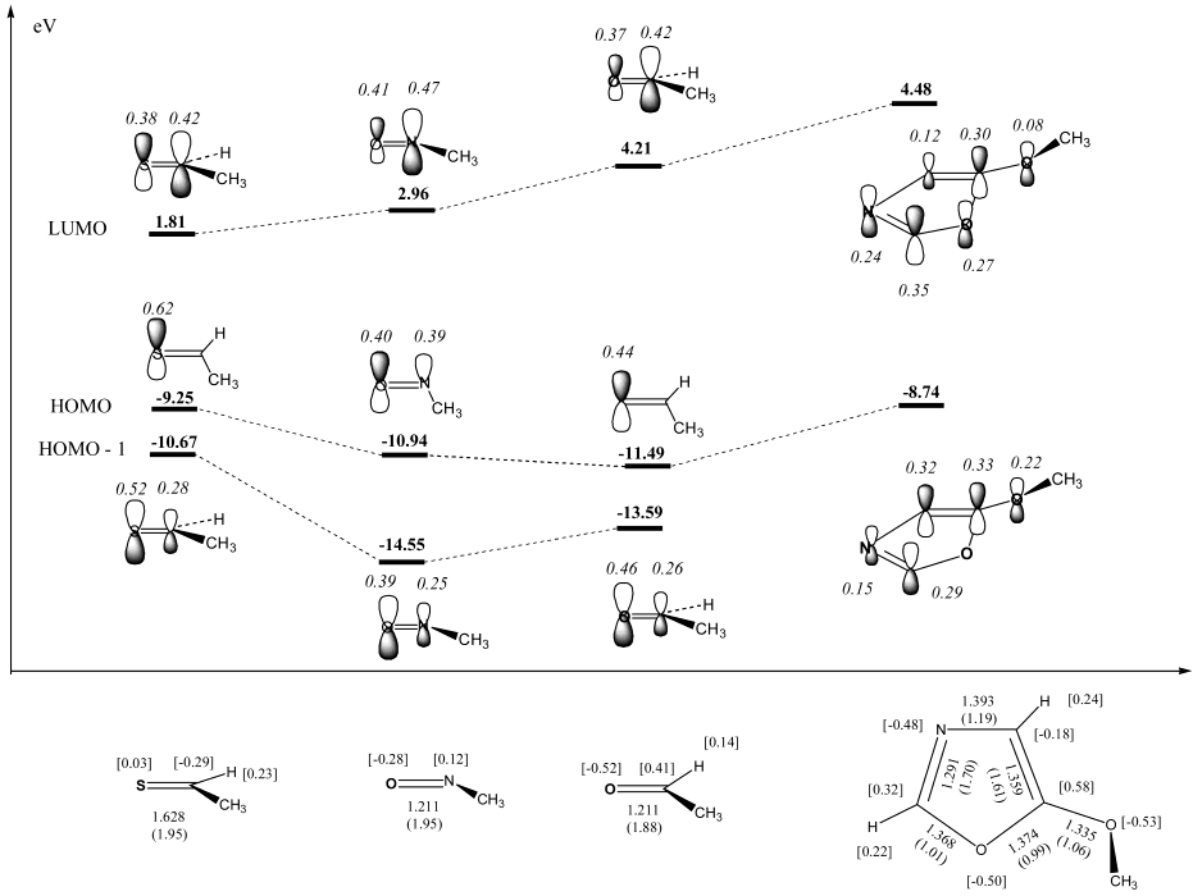

FIGURE 1. Frontier molecular orbitals and geometries of 5-methoxyoxazole (MOX) and heterodienophiles. Solid values are orbital energies (in eV). The italic values are orbital coefficients (2P for C, N, O and 3P for S). Bond lengths are in angstroms (bond orders are provided in parentheses). NPA charges are in brackets.

observed a similar endo preference for the DA reactions involving thioaldehydes as heterodienophiles. Steric effects are responsible for the lower stability of the exo TS **5** relative to the endo TS **1**, as judged by the closer distances of $(C_{10})-H\cdots H-(C_2)$ and $C_{10}\cdots H-(C_2)$ in **5** (2.404 and 2.777 Å, respectively) than those in **1** (2.651 and 3.028 Å, respectively).

Even though the DA reactions in manifold A are exothermic, the DA adducts **2** and **6** are less stable than the reactants of MOX and $CH_3CH{=}S$ in terms of free energy, due to the entropy penalties accompanying the DA processes. This is likely the reason 5-alkyl and 5-unsubstituted oxazoles cannot trap thioaldehydes due to the lack of a subsequent exothermic RORC step. Nevertheless, for 5-alkoxyoxazole, this adversity can be released via the RORC step to furnish 3-thiazoline, which is now more stable than the reactants by about 32 and 20 kcal/mol in terms of ΔE_0 and ΔG_{298}, respectively. IRC calculations indicate that the RORC is a one-step reaction, where two bond cleavages (the C_2-O_1 and the C_5-S bonds) and one bond formation (the C_4-S bond) occur in a concerted fashion without involvement of a zwitterionic intermediate. Bond orders in the RORC TS **3** show that the bond-forming and breaking processes have proceeded to a large extent (see Figure S5). Owing to the concerted feature of the DA and RORC reactions, we regard that during the reaction there is no involvement of zwitterionic species as was proposed by Vedejs.[3]

The calculated activation barriers for these RORC steps are not high, 14.0 and 15.4 kcal/mol for converting **2** to **4** and **6** to **8**, respectively. It is also found that the RORC TSs **3** and **7** lie lower on the potential energy surface than the DA TSs **1** and **5**, suggesting that the rate-determining step in both the A-endo and the A-exo paths is the DA reaction. Activation energies of less than 10 kcal/mol for the DA rate-determining step not only mean that reaction I can proceed readily but also suggest that the final ratio of *trans*- and *cis*-3-thiazolines is determined by the relative stabilities of TSs **1** and **5**. The 0.5 kcal/mol stability of **1** over **5** in terms of ΔG_{298} implies that the product distribution has a trans/cis ratio of 3-thiazoline by about 2.3/1, a value very close to the experimental observation of 2.5/1 for the reaction of CH_3-$CH{=}S$ with 2-phenyl-5-methoxyoxazole.[3] Even though Vedejs[3] did not mention which product is dominant, the calculations suggest that *trans*-3-thiazoline is the major product, which originated from the preference of the endo DA TS **1** over the exo DA TS **5** in the initial step of the reaction.[25−27]

Therefore, the above theoretical investigation of reaction I reproduces the experimentally observed regiochemical feature of exclusively generating 3-thiazoline via manifold A. The small stereochemical preference of

(24) Vedejs, E.; Stult, J. S.; Wilde, R. G. *J. Am. Chem. Soc.* **1988**, *110*, 5452.

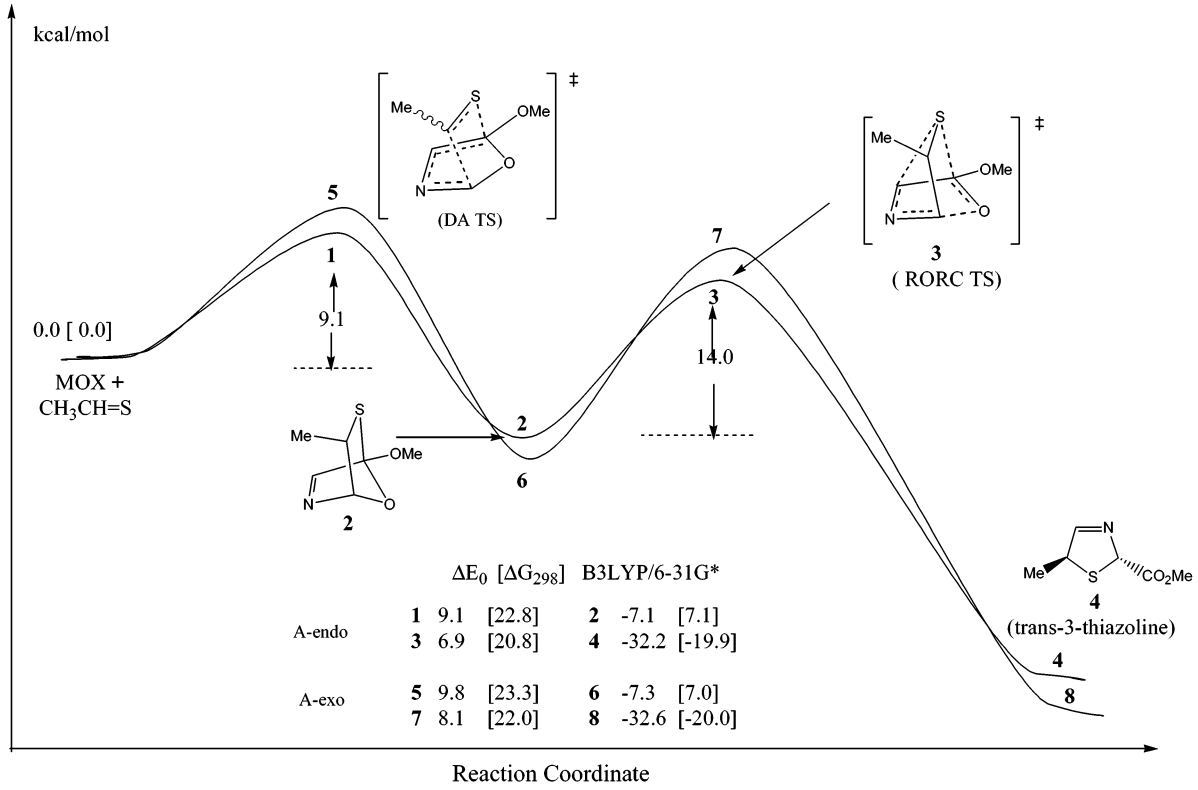

FIGURE 2. The potential energy surface for reaction II between MOX and thioaldehyde $CH_3CH{=}S$ computed at the B3LYP/6-31G* level.

yielding *trans*-3-thiazoline over *cis*-3-thiazoline, originating from the preference for the endo DA reaction in this course, is rationalized as well.

3.2. Reaction II (MOX + $CH_3N{=}O$).

The favorite path of reaction II is the A-endo path, which is shown in Figure 3. The computed structures involved in this path are given in Figure S8 of the Supporting Information, together with the exo DA TS **23** of the A-exo path. It is shown that reaction II also begins with a concerted but asynchronous DA step, which has a significant preference for endo DA TS **17** over exo DA TS **23** by 6.0 kcal/mol (10.3 vs 16.3 for **17** and **23**, with respect to MOX plus $CH_3N{=}O$). Such a large preference of endo TS over exo TS was also observed in the reaction between 1,3-butadiene and $H{-}N{=}O$ (8.1 kcal/mol at the MP2/6-31G* level) by Houk.[23] We attribute the higher energy of the exo DA TS **23** relative to the endo DA TS **17** to the additional repulsion between the lone pair of the dienophile's nitrogen atom (N_9) and the π electrons in the diene fragment ($C_2{=}N_3{-}C_4{=}C_5$) in the exo TS. DA adduct **18** also favors the endo conformation to avoid such adverse repulsion, as shown by the calculations that the exo conformer of DA adduct **18** is higher in energy than its endo counterpart by 0.4 kcal/mol.

Like the DA reaction between thioaldehyde and MOX, the DA reaction between nitrosomethane and MOX in the present case is also exothermic (−4.0 kcal/mol) and endergonic (10.1 kcal/mol in terms of ΔG_{298}). However, distinct from reaction I, the DA adduct **18** here is converted to the final product **22** through a two-step rather than a one-step process, with a zwitterionic intermediate (ZW-IN) **20**, ring-opening (RO) TS **19**, which has the $C_2{-}O_1$ and $C_5{-}O_8$ bonds breaking to a significant extent, and ring-closing (RC) TS **21**, which corresponds to the $C_4{-}O_8$ bond formation transition state (Figure S8). The existence of ZW-IN **20** is attributed to the conjugation effect introduced by the nitrogen atom N_9, as manifested by the short bond length (1.326 Å) and large bond order (1.40) of its $C_2{-}N_9$ bond (for comparison, the $C_2{-}N_9$ bond in **18** is a single bond with bond length and bond order of 1.496 Å and 0.94, respectively). The conjugation can delocalize electrons in the whole system and consequently stabilize the zwitterionic intermediate. On the contrary, in reaction I, the bridge atom connecting

(25) Vedejs speculated that another DA adduct **10** generated in manifold B is probably in equilibrium with DA adducts **2** and **6** generated via manifold A before the latter two adducts are converted to the final 3-thioazolines. Figure S4 shows that this is impossible kinetically, since the activation energy needed for the generation of **10** is 17.5 kcal/mol, about 8 kcal/mol higher than those (9.1 and 9.8 kcal/mol) of the DA reactions in the manifold A. In addition, manifold B is certainly the dead-end path, since its [4 + 2] adduct **10** is less stable than the reactants by about 11.2 kcal/mol in terms of ΔG_{298} (see Supporting Information for the energies and structures of DA TS **9** and adduct **10**).

(26) An interesting feature worthy of note is that the *cis*-3-thiazoline **4** is more stable than *trans*-3-thiazoline **8** by about 0.4 kcal/mol. So is the 3-oxazoline which has the *cis*-3-oxazoline being more stable than *trans*-3-oxazoline by about 0.4 kcal/mol, too. The reason for this cis preference is probably the electronic attraction between the two groups.

(27) There is another possible path involving a pseudopericyclic reaction converting 5-alkoxyoxazoles to ylides (a process analogous to the Cornforth rearrangement),[28] which then react with thioaldehydes via a [3 + 2] dipolar addition reaction to generate the final products.[3,5a] This path can be easily excluded, owing to the high activation energy of 30.2 kcal/mol needed to generate the ylide **16** (see Figure S7 in Supporting Information). In terms of free energy, the pseudopericyclic TS **15** is still higher than the rate-determining TS **1** in the manifold A by about 8 kcal/mol. Furthermore, the ylide is a species lying higher in energy than the reactants by around 20.6 kcal/mol, suggesting that the backward ring-closing reaction converting ylide to oxazole is more efficient.

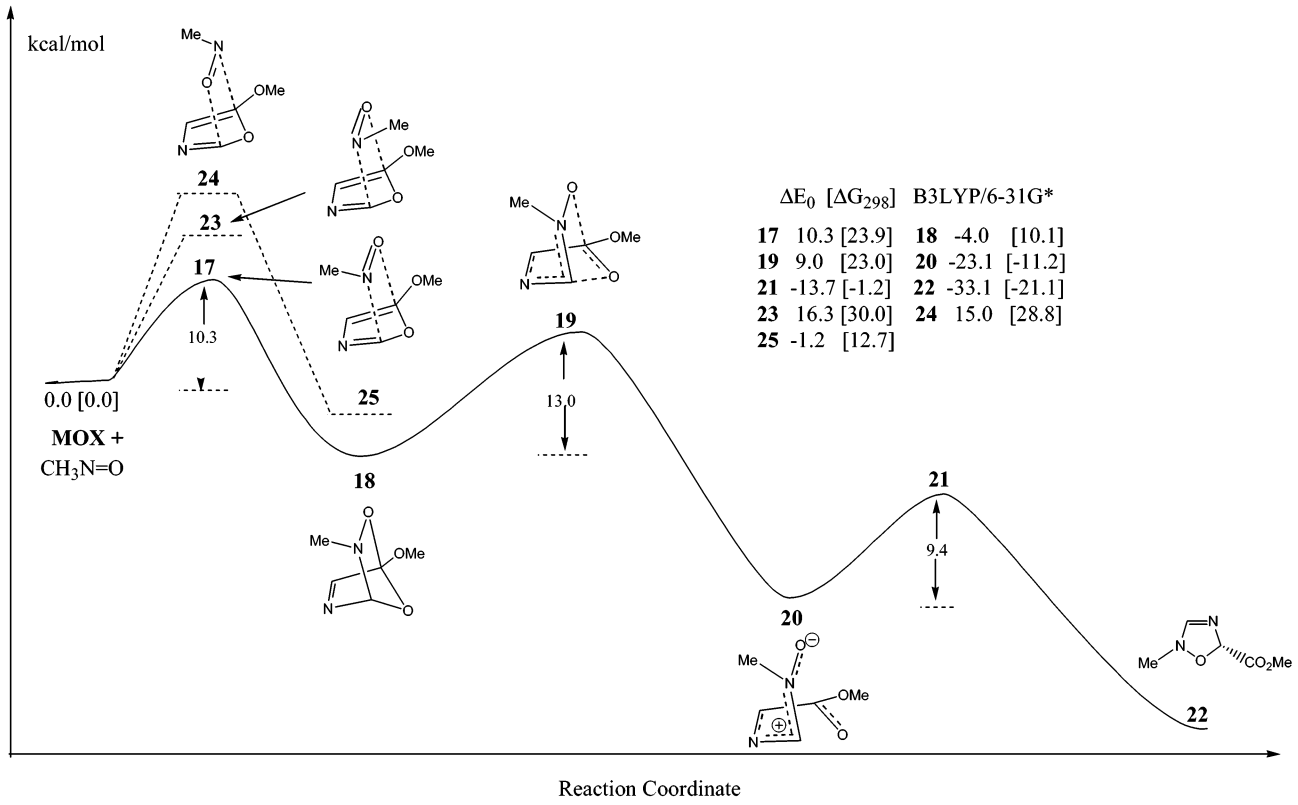

FIGURE 3. The potential energy surface for reaction II between MOX and $CH_3N{=}O$ computed at the B3LYP/6-31G* level.

the MOX and the thioaldehyde fragment in DA adduct **2** is a carbon atom, which prevents the conjugation effect, so that a zwitterionic species cannot be stabilized.

Conjugation also exists in the ring-opening TS **19**, as indicated by a bond order of 1.25 for its $C_2{-}N_9$ bond. This is the major contribution for the low activation barrier of 13.1 kcal/mol for converting DA adduct **18** to ZW-IN **20**. The RC step is also very efficient due to the 9.4 kcal/mol activation energy for converting the zwitterionic intermediate **20** to 1,2,4-oxadiazoline **22**.

The potential energy surface in Figure 3 shows that reaction II is not only very exothermic (−33.1 kcal/mol) but also very facile, since the rate-determining step is the DA reaction, which has activation energy of 10.3 kcal/mol.

In summary, reaction II between nitroso compounds and MOX intrinsically favors the A manifold to furnish 1,2,4-oxadiazoline via DA, RO, and RC steps.[12]

3.3. Reaction III (MOX + $CH_3CH{=}O$).

The potential energy surfaces for all the A-endo and A-exo paths of reaction III are given in Figure 4. The geometries of these stationary points are given in Figure S10 of the Supporting Information.

Figure 4 shows that the manifold A leading to the formation of 3-oxazolines is the most favorable, wherein concerted but asynchronous DA reaction is followed by a RORC process, very similar to reaction I. The structures of the TSs and the intermediates in the manifold A of reaction III warrant no further comments here, since they are very similar to their counterparts in reaction I, except for the differences caused by O_8 and S_8 atoms in the two reactions.

Energetically, even though the DA reaction in the most competitive manifold A possesses slightly higher activation energies of 21.2 and 21.8 kcal/mol for A-endo and A-exo paths, compared to reactions I−II, the bottleneck that prevents reaction III from occurring is the RORC step, in which the RORC TSs **28** and **32** lie about 30.5 and 31.9 kcal/mol above the separated reactants. Taking into account the entropy contributions, reaction III has a 44.0 kcal/mol activation free energy in the gas phase. This is the main reason the thermal reaction condition cannot be applied to the reactions of 5-alkoxyoxazoles and aldehydes.

Two sources contribute to the relatively high energy of the RORC TSs. The first one is due to the endothermic DA processes producing adducts **27** and **31**, which both lie above the reactants by about 5 kcal/mol. (The DA reactions are exothermic in reactions I and II, by contrast.) The second and the most important source is the RORC reactions themselves, which need activation energies of 25.1 and 27.3 kcal/ mol in the A-endo and A-exo paths to transform the DA adducts to the final *trans*- and *cis*-3-oxazolines, respectively. Here we can see that the A-endo path is more favorable than the A-exo path by about 1.4 kcal/mol (**28** vis **32**), implying that the *trans*-3-oxazoline would be the dominant product if the thermal reaction could happen. Again, an endo preference of 0.6 kcal/mol in the DA reaction is found and the reason is attributed to steric effects, as manifested by the shorter distances of $(C_{10}){-}H{\cdots}H{-}(C_2)$ and $C_{10}{\cdots}H{-}(C_2)$ in exo DA TS **30** (2.617 and 2.838 Å) than those in endo DA TS **26** (2.910 and 3.005 Å).

In summary, reaction III between acetaldehyde and MOX intrinsically favors manifold C to generate 3-oxazoline, even though this reaction cannot be conducted under thermal reaction conditions due to the 30.5 kcal/mol activation energy needed.

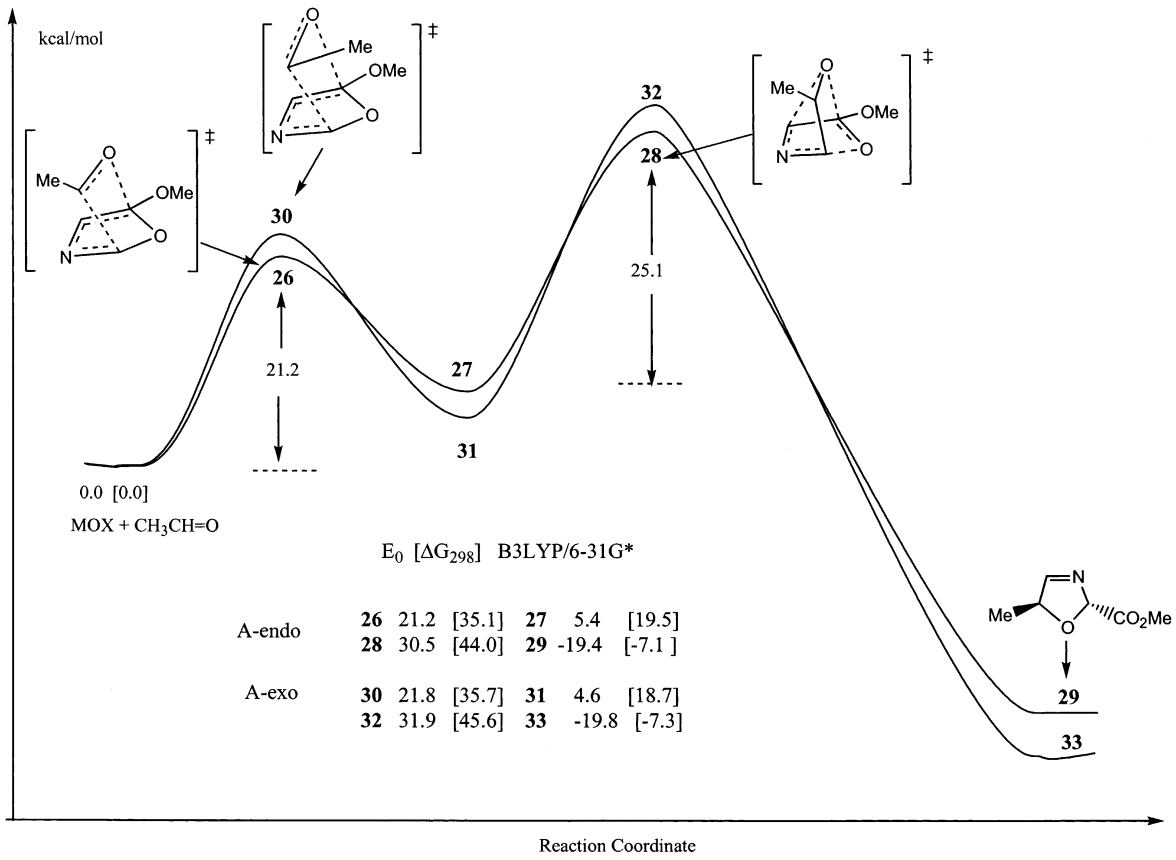

FIGURE 4. The potential energy surface for reaction II between MOX and aldehyde $CH_3CH{=}O$ computed at the B3LYP/6-31G* level.

4. Discussion

4.1. Regiochemistry of the DA Reactions in Reactions I−III.

It is important to note that for reactions I−III the DA steps involved in the A manifold have lower activation energies than their counterparts in manifolds B and C (see Figures S4, S9, and S11),[29] suggesting that there is no involvement of DA adducts of the B manifold during the reactions I and II.[24] However, the relatively high activation energies of the DA reactions in the B manifold compared to their counterparts in the A-endo paths are opposite to FMO theory,[30] which suggests that the former TSs should be more efficient than the latter, since the TSs in the B manifold involve the addition of C_5 to a Y atom of $CH_3Y{=}X$, both of which have the largest orbital coefficients in the MOX's HOMO and $CH_3Y{=}X$'s LUMO, respectively (see Figure 1 and Scheme 7). However, the observed regiochemistry is consistent with the electron-donating effect of the methoxy substituent.

The following two factors can be invoked to reconcile this contradiction. The first factor, which destabilizes DA TSs in the manifold B more than those in the A-endo path, is the repulsion of the lone pair of the X atom in the dienophile $CH_3Y{=}X$ with the π electrons in the $N_3{=}$

SCHEME 7

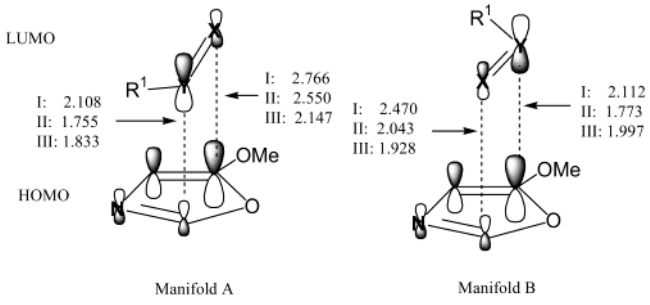

C_4 fragment as well as with the lone pair of the O_1 atom in MOX, since the DA TSs in the B manifold have shorter $C_2{-}X$ distances (2.470, 2.043, and 1.928 Å in reactions I−III, respectively) than $C_5{-}X$ distances of their counterpart DA TSs in the manifold A (2.766, 2.250, and 2.147 Å in the reactions I−III, respectively). The reaction energy of the DA reaction is the second factor. According to the Bell−Evans−Polanyi principle,[31] for similar reactions, the more exothermic process will have the lower activation energy. The DA reactions in the B manifold have lower reaction energies than those in the A-endo path (A manifold, −7.1, −4.0, and 5.4 kcal/mol; B manifold, −3.1, −1.2, and 9.6 kcal/ mol for the reactions I−III, respectively), suggesting that the DA reactions in the A manifold are more exothermic than those in the B

(28) (a) Turchii, I. J.; Dewar, M. J. S. *Chem. Rev.* **1975**, *75*, 420. (b) Taylor, E. C.; Turchii, I. J. *Chem. Rev.* **1979**, *79*, 181.

(29) It is understandable for high activation energies involved in the C manifold, since this reaction needs a zwitterionic MOX; on the other hand, the TS involved has to break an additional $C_2{-}O_1$ bond.

(30) Fleming, I. *Frontier Orbitals and Organic Chemical Reactions*; Wiley: London, 1982.

(31) Dewar, M. J. S. *The Molecular Orbital Theory for Organic Chemistry*; McGraw-Hill: New York, 1969.

manifold, and consequently, higher activation energies are needed for the latter DA reactions.

4.2. Energetics of the Three Different DA Reactions in Their Preferred A-Endo Paths of Reactions I−III.

The order of the activation barriers of the DA reactions for the reactions I−III is I (9.1 kcal/mol) < II (10.3 kcal/mol) < III (21.1 kcal/mol), in parallel with the order of the LUMO orbital energies of the dienophiles: $CH_3CH{=}S$ < $CH_3N{=}O$ < $CH_3CH{=}O$ (Figure 1). This is consistent with the prediction by FMO theory for the normal-electron demand DA reactions. Charge analysis also reveals charge transfer from the oxazole fragments to the dienophile moieties in the DA TSs (0.21, 0.33 and 0.29 units in reaction I−III, respectively), as shown in Table S1 of Supporting Information. The stronger C=O bond than the C=S and N=O bond is another reason for the high activation barrier of the DA reaction of reaction III. This is also the reason the DA step in reaction III is endothermic.

4.3. Origin of the Different Activation Barriers for the RORC or RO Processes.

As per our expectations, the inertness of aldehyde to 5-alkoxyoxazoles is not due to the sluggish DA step but mainly due to the RORC step. A question remaining unanswered is, why is the barrier height of this step about 25 kcal/mol, while the corresponding activation barriers for the reactions I and II are only 14 and 13 kcal/mol, respectively?

The origin of the difference is apparently related to the relative abilities of the $CH_3Y{=}X$ fragments to stabilize the zwitterion-like RORC or RO TSs, where the dienophile fragments possess negative charges (0.21, 0.37, and 0.34 in RORC or RO TSs **3**, **19**, and **28**, respectively; see Table S1). Electron-withdrawing groups on the dienophile fragment and electron-donating groups on the oxazole fragment are expected to stabilize these TSs and consequently lower the activation energy. Given the same oxazole fragments in these TSs, the more efficiently the Y=X stabilizes the anionic $CH_3Y{=}X$, the lower the activation energy would be for the RORC or RO TSs. It is known that CH_3CHS^- is much more stable than CH_3CHO^-, since the large S atom has higher polarizability than the small oxygen atom.[32] This is evident in Houk's calculations,[28a] which indicate that thiyl (−SH) is more efficient than hydroxyl (−OH) in stabilizing methyl anion by about 15.1 kcal/mol (B3LYP/ 6-31+G*), comparable with the 11 kcal/mol difference in activation energy difference for the RORC steps of reactions I and III. Another related support is the experimental observation that a thioalkoxy substituent is more efficient than an alkoxy substituent in accelerating anionic oxy-Cope rearrangements.[33]

Although in the RO TS **19** of reaction II the less efficient oxygen atom is used to stabilize the negative charge there, a conjugation effect introduced by the nitrogen atom of $CH_3N{=}O$ is applied to compensate for this inefficiency, as indicated by the bond length (1.361 Å) and bond order (1.25) of the C_2-N_9 bond in TS **19** (see Figure S8). This is the reason intermediate **20** is located for reaction II. On the contrary, this conjugation is impossible for reaction III and therefore high activation energy is needed.

5. Conclusions

In summary, our calculations have unveiled that the model reactions of I−III (Scheme 4) occur in a very similar fashion. The first step for all of them corresponds to a normal-electron demand DA reaction involving addition of the C_2 and C_5 atoms of 5-methoxyoxazole (MOX) to the Y and X atoms of the $CH_3Y{=}X$ of the heterodienophiles to generate [4 + 2] adducts (see Scheme 5). The adducts in reactions I and III are then transformed to final 3-thiazoline and 3-oxazoline, respectively, via a concerted ring-opening−ring-closing step. By contrast, for reaction II this conversion is a stepwise process involving a ring-opening reaction and a ring-closing reaction. Conjugation introduced by the nitrogen atom in $CH_3N{=}O$ is responsible for this stepwise transformation, since the zwitterionic intermediate connecting the RO and RC steps can be stabilized by this effect.

Both reactions I and II can be conducted under thermal reaction conditions because their DA reactions acting as rate-determining steps have activation energies of 9.1 and 10.3 kcal/mol. However, the thermal reaction conditions cannot be applied to reaction III, not due to its DA reaction, which has activation energy of 21.2 kcal/mol, but due to its RORC step, which has a transition state lying about 30.5 kcal/mol higher than the reactants. This almost insurmountable activation barrier is attributed to the less stable DA adduct caused by the endothermic DA reaction in III (the DA reactions in I and II are exothermic) and the high activation barrier of 25.1 kcal/mol needed to convert the DA adduct to final product on the other. By contrast, the RORC reaction in reaction I has a barrier of only 14.0 kcal/ mol. The lower activation barrier of the RORC step in reaction I than that in reaction III is due to the stronger stabilizing ability of the sulfur atom to the anionic moiety in its RORC TS than the aldehyde's oxygen atom. The inferior stabilizing ability of oxygen in reaction II, on the contrary, is compensated by the conjugation effect caused by the nitrogen atom of $CH_3N{=}O$, leading to a 13.1 kcal/mol activation barrier for the RO step.

Acknowledgment. We are grateful to the Research Grants Council of Hong Kong for financial support of the work. Y.-D.W. also thanks the Croucher Foundation for a Croucher Senior Research Fellowship award. Z.-X.Y. is indebted to Drs. A. G. Leach and B. N. Hietbrink for fruitful discussions. We are especially indebted to the referees who gave particularly construc-tive suggestions for the improvement of the manuscript.

Supporting Information Available: The HF/3-21G* calculations for reactions I−III and the DFT-calculated structures, Cartesian coordinates, E_{ele}, H_{298}, G_{298}, ZPE, and other thermodynamic parameters for all the structures. This material is available free of charge via the Internet at http://pubs.acs.org.

JO026330E

(32) (a) Lehn, J.-M.; Wipff, G. *J. Am. Chem. Soc.* **1976**, *98*, 7498. (b) Borden, W. T.; Davidson, E. R.; Andersen, N. H.; Denniston, A. D.; Epiotis, N. D. *J. Am. Chem. Soc.* **1978**, *100*, 1605. (c) Schleyer, P. v. R.; Clark, T.; Kos, A. J.; Spitznagel, G. W.; Rohde, C.; Arad, D.; Houk, K. N.; Rondan, N. G. *J. Am. Chem. Soc.* **1984**, *106*, 6467.

(33) (a) Haeffner, F.; Houk, K. N.; Reddy, Y. R.; Paquette, L. *J. Am. Chem. Soc.* **1999**, *121*, 11880. (b) Paquette, L. A.; Reddy, Y. R.; Haeffner, F.; Houk, K. N. *J Am. Chem. Soc.* **2000**, *122*, 740. (c) Paquette, L. A.; Reddy, Y. R.; Haeffner, F.; Houk, K. N. *J Am. Chem. Soc.* **2000**, *122*, 10788.

(34) Yu, Z.-X; Wu,Y.-D. *J. Org. Chem.* **2002**, *67*, 421.